Effect of ER70s Filler Metal on Mechanical Properties and Corrosion Behaviour of Low Carbon Steel Produced by Gas Metal Arc Welding

Mohd Fauzi Mamat[a,*], Siti Nadirah Mohd Syukor[a], Mohd Faiz Mohd Bokhadi[b], Rohah Ab. Majid[c], Lailatul Harina Paijan[a], Mohd Basri Ali[a] Mohd Hadzley Abu Bakar[a] and Mohd Idain Fahmy Rosley[d]

[a]Faculty of Industrial and Manufacturing Technology and Engineering, Universiti Teknikal Malaysia Melaka (UTeM), Kampus Teknologi, Hang Tuah Jaya, 76100 Durian Tunggal, Melaka, Malaysia
[b]Group Technical Inspection (GTI) Sdn. Bhd. / IFOCS EngTech Sdn. Bhd. Jln Elektron U16/EDenai Alam, 47000 Shah Alam, Selangor
[c]Faculty of Chemical Engineering and Energy Engineering, Universiti Teknologi Malaysia, 81310 UTM Skudai, Johor, Malaysia
[d]Faculty of Mechanical Technology and Engineering, Universiti Teknikal Malaysia Melaka (UTeM), Kampus Teknologi, Hang Tuah Jaya, 76100 Durian Tunggal, Melaka, Malaysia
*Corresponding author. Tel.: +6012-3471869; fax: +606-2701064; e-mail: fauzi.mamat@utem.edu.my

ABSTRACT

The Gas Metal Arc Welding (GMAW) process is leading the way in arc welding process growth because it is more efficient, economical, and of high quality. The effects of ER70s filler metal on mechanical properties and corrosion behaviour in low carbon steel with a base metal thickness of 12 mm are investigated in this study using robotic gas metal arc welding (GMAW). After the welding process, the quality, microstructure, and micro-hardness of each specimen were measured and the effect was studied. The immersion test was studied using weight loss and corrosion rate measurements for 1, 2, 4, 6, and 8 weeks in the absence and presence of 3.5wt. % NaCl. As a result, the microstructure displayed the different grain boundaries of each parameter that affected the welding parameters. Scanning electron microscopy (SEM) and energy dispersive spectroscopy (EDS) are used to characterise the surface morphology and pitting areas on the welded substrate. The corrosion rate of the welded sample immersed in 3.5wt. % medium was higher than in the absence of NaCl. The SEM results revealed that NaCl played an aggressive role in inducing the corrosion process and producing significant pits on the welded joint, particularly in the HAZ area. This research may provide a significant understanding of how the welding process, filler metal, and low carbon steel metal caused corrosion behaviour in the marine environment, particularly for oil and gas applications.

Keywords: *Welded joint, Micro hardness, Heat-affected zone, Corrosion rate*

1. INTRODUCTION

Low carbon steels are used in a wide range of industrial applications due to their mechanical properties, ease of welding, availability, and low cost [1]. Low carbon steels are widely used in the marine and offshore industries, including shale gas energy, for ships, plants, and pipe construction. However, drawbacks such as low hardness and poor corrosion resistance limit their application potential, particularly in the oil and gas application [1, 2].

Welding is a critical process in steel fabrication and assembly. It has several advantages over other joining processes and technologies, including the ability to permanently bond complicated shapes and to weld very thin materials [3-4]. Welding is especially important in many industries, including oil and gas, petrochemical, and automotive. Welding imperfections may occasionally be introduced in existing weldments after the welding process for a variety of reasons [2-5].

The GMAW process is leading the way in the development of the arc welding process, as it is more efficient, cost-effective, and of high quality. Metal Inert Gas (MIG) is another name for GMAW, which is a process that consists of heating, melting, and solidifying parents metals and a filler metal (wire electrode) material in a controlled fusion zone by passing a heat source to form a joint between the two parents' metals [6]. The continuous wire electrode from an automatic wire feeder is melted by the internal resistive power and heat from the welding arc and fed through the contact tip within the welding torch. Heat is measured from the melting electrode's end to the molten weld pools, as well as the molten metal that is transferred to the weld pools [6-8]. Arc welding current, arc voltage, welding speed, torch angle, free wire length, nozzle distance, welding position and direction, and gas flow rate are the following welding parameters. [6-8]. The highest available welding conditions are determined by a combination of factors such as base metal type, welded part geometry, and welding process [6-9]. During service, the welded joint is exposed to environmental factors such as marine environments, which influence corrosion issues.

The oil and gas sectors are prone to corrosion because of their complicated operating circumstances, which include high pressure, high temperatures, multiphase flow, high pH values, and ion concentrations [10]. The microstructure and mechanical characteristics of the welded zone are very different from the base metal's due to the welding process. Owing to the welding process, the HAZ area exhibits a weaker component following rapid head cooling, and the

corrosion behavior is influenced by the existence of flaws and discontinuities such undercuts, cracks, and other features. Because of this, it is anticipated that the welded zone and HAZ area will exhibit different corrosion behavior from other areas in corrosive environments [10–12].

Despite existing work on the welding of low carbon steel 12mm plate, an investigation of the effects of the GMAW process, in particular, on the microstructure and corrosion performance of welded structures in 3.5wt. % NaCl medium for 1 to 8 week immersion times is required. Following the welding process, non-destructive testing and visual inspections were performed. Microstructure analysis, scanning electron microscope studies equipped with energy dispersive X-ray spectroscopy (SEM-EDS) for surface morphology studies, and chemical analysis of corrosion products are all performed.

2. MATERIAL AND METHODS

The current study focused on a profitable low carbon steel plate. The material was in the form of a 12 mm thick plate with a ferrite-pearlite structure when it was received. The chemical composition of the base and the filler used is shown in Table 1. The base material used in this study for gas metal arc welding (GMAW) was low carbon steel plates with dimensions of 100 mm × 50 mm × 12 mm, and the filler was ER70s electrode. The type of joint used for this project is a butt joint, and the butt joint geometry is a single V with an angle of 60ºC, as seen in Figure 1.

Table 1 Chemical composition (wt. %) of the base metal and filler used

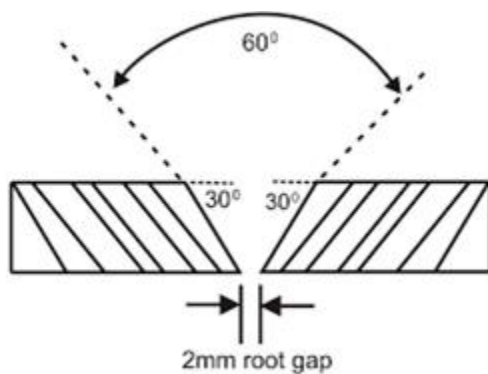| Alloy element	C	Si	Mn	P	S	Cr	Ni	Cu	Fe
Base metal	0.17	0.18	0.62	0.02	0.02	0.10	0.07	0.22	Balance
Filler (ER70s)	0.10	0.24	0.52	0.02	0.01	0.04	0.10	0.06	Balance

Figure 1. Single V Joint preparation.

The welded pieces were subjected to X-ray radiography after the welding process. Faulty and poorly welded pieces were not accepted. Microstructure and mechanical test analysis were performed on welded pieces that were free of defects or faults. To reduce the amount of heat generated during the cutting process, both test samples were cut into smaller pieces of approximately 50 mm × 10 mm × 12 mm using EDM wire cut. Before the test, all of the specimens were thoroughly cleaned. The cleaning procedure included grinding with SiC paper from 200 to 1200 grit, finishing with a grinding machine, and etching in a 2% Nital solution for microstructure analysis. This would make identifying the HAZ, fusion zone, and base metal area easier.

A Nikon optical micrograph was used for microstructure analysis of low carbon steel weld joints. Micro-hardness tests were performed on the cross section of the welded joint along 3 mm from the top, center, and bottom surfaces at 0.5 to 1 mm intervals with 9.81 N loads, as shown in Figure 2. The Shidmadzu HMV-2T micro-hardness testing machine was employed.

Figure 2. Depths of bead for micro-hardness measurement.

Immersion testing was performed in accordance with ASTM G1–03. Welded specimens with dimensions of 50 mm × 10 mm × 12 mm were immersed in a 5 liter container containing 3.5wt. % NaCl medium for 1, 2, 4, 6, and 8 weeks. During the testing period, the solution was not replenished. After every immersion test, the samples were taken out of the 3.5 weight percent NaCl solution and soaked in accordance with ASTM G31 to eliminate corrosion products. Before and after cleaning, the image was captured for the purpose of visual assessment. The samples were then dried using high pressure air, washed with ethanol, and weighed. The following formula was used to determine the corrosion rate:

$$\text{Corrosion Rate (CR)} = \frac{K \times W}{A \times T \times D} \quad (1)$$

Where CR is the corrosion rate (mm/ year), constant, K = 8.76×10^4, W is the mass loss (gram), A is the surface area (cm^2), exposed to the corrosive media, T is the exposure time (hour), D is the density (g/cm^3). Scanning Electron Microscope (SEM) coupled with Energy Dispersive Spectroscopy (EDS) is used to identify the surface analysis for studying the corrosion behaviour on surface of welded joint especially at HAZ zone and between base metal and weldment

3. RESULT AND DISCUSSION

3.1 Microstructural Analysis

Microstructural analysis is performed using an optical microscope and line scanning with a SEM. The optical microscope observes three areas: the base metal, the heat affected zone (HAZ), and the weld metal. Figure 3 shows the microstructure of the sample after etching with a 2% Nital solution under an optical microscope. Under the microscope, the etching solution allows for a clearer view of the grain boundary. The sample's microstructure included pearlite and ferrite structures. The darker area is pearlite, and the brighter area is ferrite as shown in Figure 3 (a to c).
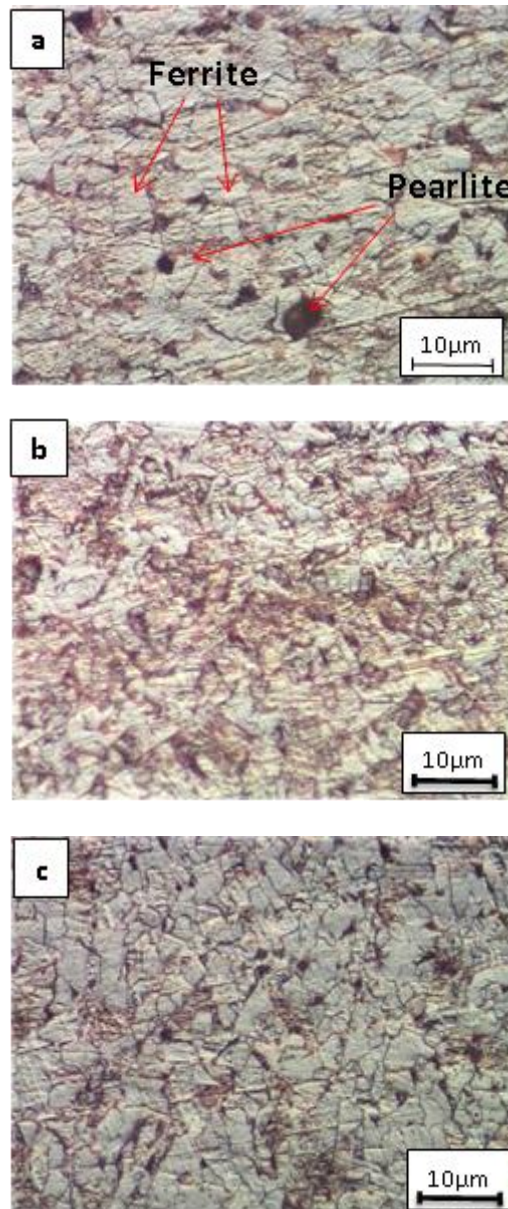
Figure 3. Microstructure of Sample under Optical Microscope (a) Base metal, (b) Heat affected zone, (c) Weld metal.

Figure 3 (b) depicts the HAZ caused by welding processes, welding currents, and weld heat input. It is clear that the welding process was influenced by the change in HAZ microstructure. This is due to these welding processes increasing welding heat input [1-5]. While in Figure 3 (c) show by using ER70s filler metal, the weld metal (WM) contains mostly acicular ferrite with a trace amount of bainite [5]. The rain boundary ferrite was also plainly seen and smaller acicular ferrite particles.

3.2 Line Scanning Analysis

Figure 4 depicts the distribution of the major alloying elements on a cross section of the ER70s filler metal, HAZ, and base metal using the line scanning method and a SEM. Carbon, oxygen, magnesium, silicon, iron, and copper were all present in the welded sample. According to W. Thai et al. [2] the chemical composition of the base material differs significantly from that of the weld. The elements in the weld and the base material inter-diffused due to the welding process's heat action.
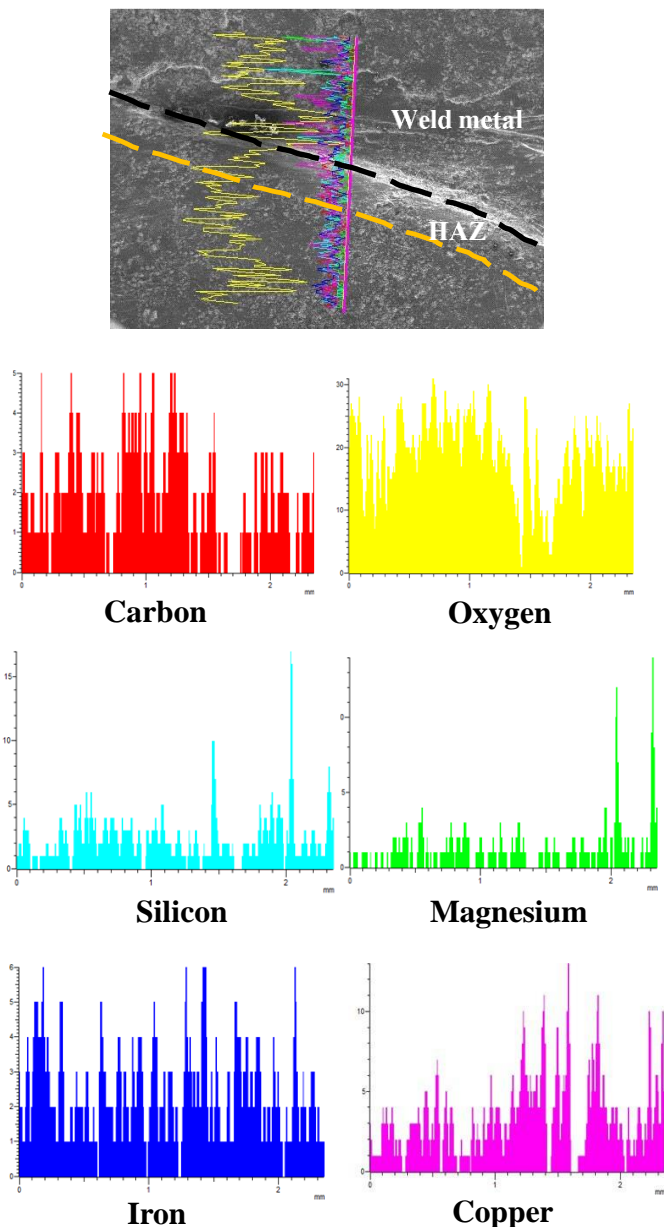
Figure 4. EDS line scan demonstrating alloying element variation across the interface base material to weld metal interface.

3.3 Micro-Hardness Study

The micro-hardness measurement was obtained across three main zones: base metal, HAZ area, and weld metal. The micro-hardness was determined at three different depths: top, center, and bottom. The hardness of the weld nugget region ranged from 139 to 145 HV1, and the

difference in hardness across the thickness direction in the weld nugget was bordering. Since this area was close to the weld pool, the hardness of the LCS/HAZ region adjacent to the weld nugget was higher than that of the nugget region, registering values in the range 148 - 153 HV1It was discovered that the parent LCS had a sharp hardness gradient between the parent and the LCS/HAZ area, with a hardness range of 134 to 173 HV1. Perceptible fluctuations in the weld nugget's grain size do not appear to have had a substantial effect on its hardness, as indicated by the consistent distribution of hardness over the section thickness [11].

Figure 5 also revealed that the bottom part of the sample has higher hardness values than the top part. The reason for this is that the top part of the bead is more exposed to rapid heat and cooling layer by layer of bead during the welding process. When heated, it softens, resulting in low hardness values. The sample depth, which was located in the center, was made up of average micro-hardness values.

Figure 5 shows that the heat affected zone (HAZ) has a high micro-hardness value when the micro-hardness value is examined through the three areas of base metal, HAZ, and weld metal. It is due to the carbon content of the weld metal moving or migrating to the HAZ area during the welding process, so when the area has more carbon contents, it is more hardened.
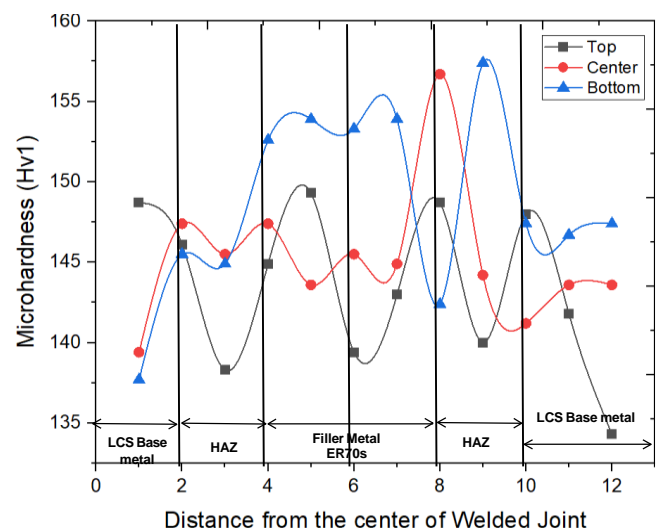

Figure 5. Micro Hardness profile at cross section of welded joint.

3.4 Visual Inspection

Based on Tables 2 and 3, they demonstrated the condition of each sample after the immersion test through visual inspection before and after cleaning the corrosion product. Following the immersion test, there is a reddish brown deposit of substances at the welded joint. This rusts, indicating that corrosion has occurred at the welded joint. As it occurs between the same metals, the type of corrosion is general corrosion. The thicker the rusts deposited at the welded joint, the longer the duration of immersion. Corrosion occurred as a result of the reaction of oxygen and iron in water or moisture in the air to form iron oxide.

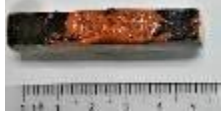**Table 2** Sample Immersed without NaCl Solution

Weeks	After Immersion	After Cleaned
1		
2		
4		
5		
6		

Table 3 Sample Immersed in 3.5% of NaCl Solution

Weeks	After Immersion	After Cleaned
1		
2		
4		
6		
8		

Table 3 shows the samples that were immersed in a 3.5 wt. % sodium chloride (NaCl) solution. When immersed in NaCl solution, more iron oxide is deposited on the sample than when immersed in fresh water (without NaCl). The salt NaCl accelerated the rusting of low carbon steel because electrons move more easily in NaCl solution than in distilled water. The layer of corrosion products developed because of the dissolved salts, which typically accelerate the rate of corrosion. Additionally, after one to eight weeks of immersion testing, the layer of corrosion products that forms on the welded junction steadily thickens. Additionally, it shows that after 8 weeks, the corrosion product's thickness is higher than it was during the 1-week immersion test. Compared to the base and weld metal sections, the HAZ area has a higher level of deposited corrosion product. The rough surface of the coupon indicates that it has both uniform and probably localized corrosion, which was detected when the corrosion agents were removed [11-14].

This study's findings are similar to the previous study of corrosion through visual inspection. It demonstrated the formation of various types of corrosion such as galvanic, crevice, pitting, and exfoliation corrosion. Visual inspection reveals the reddish-brown corrosion product. The description classification, which is particularly important in the study of failure, is based on the visual recognition of corrosion types [12-14].

3.5 Weight Loss and Corrosion Rate Measurement

Figure 6 (a) depicts the weight loss of each sample during the immersion test, which lasted from 1 to 8 weeks. The weight of the sample before immersion must be subtracted from the weight of the sample after immersion. According to Figure 6 (a), the weight loss of the sample is greater when immersed in the 3.5wt. % NaCl solution than when immersed in fresh water (without NaCl. It is the same case as the explanation for the visual inspection. Corrosion causes weight loss in the samples. The corrosion process that occurred in the samples was accelerated by the NaCl solution. When the sample is immersed in the NaCl solution, electrons move more easily, causing the sample to corrode faster. The corrosion rate of each sample in the immersion test is shown in Figure 6 (b). When the sample is immersed in 3.5wt. % NaCl solution, the corrosion rate is higher than when it is immersed in fresh water (without NaCl). The higher the corrosion rate, the greater the weight loss of the sample in a short period of time. The corrosion rate was dependent on the amount of sample weight loss. Figure 6 (a) for the sample immersed in fresh water (no NaCl concentration) showed that the weight loss was constant between weeks 6 and 8. The weight loss between the two weeks is not dramatic. It is not the case with the

sample that was immersed in a 3.5wt. % NaCl solution. Figure 6 (a) depicts the increase in weight loss between weeks 6 and 8.

Clearly, the presence of NaCl concentration in simulated marine environment results in higher weight loss and corrosion rate measurement when compared to immersion test due to the absence of NaCl composition with the same exposure time. This is because the presence of cloride (Cl^-) concentration created a more aggressive environment than the absence of salt. The NaCl solution is constantly immersed, which may affect the corrosion product form. In terms of general corrosion, the NaCl environment resulted in 80% more weight loss and corrosion rate than the immersion without NaCl environment [12-15]. The outer layer thickened as a result of an intermediate phase near the inner layer gradually changing into a different stable and dense oxide phase based on the corrosion process. It gets harder for chloride ions to pass through the outer layer [14]. On the other hand, the chlorides that were deposited during the first exposure step are diminished. These two effects enhance the protective impact of the rust layer and decrease the rate of corrosion at the welded connection by encouraging the creation of a dense and adherent inner layer [14–16].

This finding is similar to that of a previous study that looked into the effect of corrosion on mild steel in five different environments. When mild steel is immersed in salt water, it loses more weight than when it is immersed in fresh water (without NaCl). The results of the experiment clearly show that oxidation took place as weight losses became apparent. However, corrosion rates increased in the following order: 0.1 M hydrochloric acid, soil, salt water, fresh water, and atmosphere. The hydrochloric acid sample encountered what is known in engineering literature as chloride aggressiveness [17].
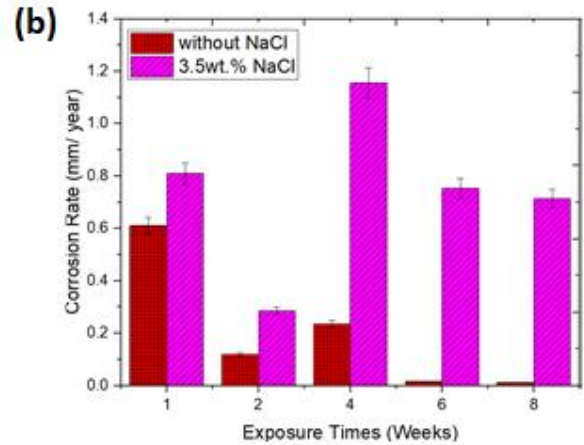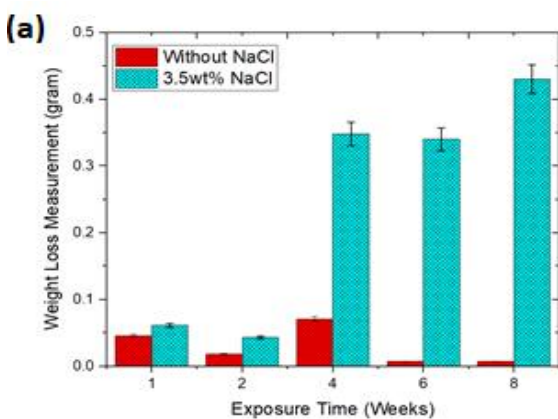

Figure 6. Immersion test results after 1 to 8 weeks for (a) Weight Loss and (b) corrosion rate measurement for welded joint.

Weldments made of carbon steel are susceptible to corrosion due to a variety of factors, including metallurgical effects like preferential corrosion of the weld metal or heat-affected zone (HAZ), geometrical aspects like stress concentration at the weld toe, or joint design, cracking, porosity, and so forth. The subjects related to corrosion of carbon steel weldments and the corrective actions that have proven to be effective in specific cases for oil and gas application are clearly defined by visual inspection, weight loss, and corrosion rate measurement. It provides useful evidence that privileged HAZ areas are more susceptible to corrosion as a result of metallurgical changes during the welding process [18].

3.6 Surface Study by SEM and EDS

Figures 7 (a) and (b) depict the surface morphology of weld metal after immersion tests in fresh water (without NaCl) for 1 and 8 weeks samples, respectively. Evidently, the type of corrosion that has occurred at the HAZ and sample weld metal is uniform corrosion. This corrosion attack spreads evenly across the entire surface of the base metal, HAZ, and weld metal. The EDS spectrum in Figure 7 (c) and (d) only contains Iron, Carbon, and Oxygen for the first week of immersion, and the amount of same composition and Si we discovered after 8 weeks of immersion test.
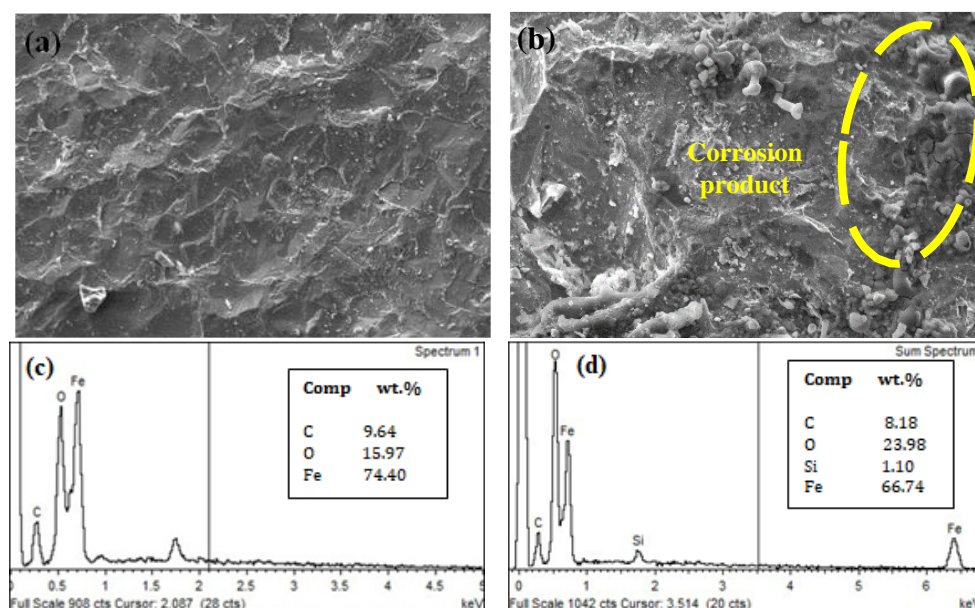
Figure 7. SEM morphology of sample immersed without NaCl solution (a) after 1 week, (b) after 8 weeks, (c) EDS analysis of sample (a) and (d) EDS analysis of sample (b).

Figures 8 (a) to (d) show the surface morphology of weld metal after immersion in 3.5wt. % NaCl solution for 1 and 8 weeks samples. Obviously, the type of corrosion that has occurred at the HAZ and weld metal of the sample is uniform corrosion, whereas localised corrosion, such as pitting, has occurred at the HAZ area. Similarly to when no NaCl is present, the corrosion attack spreads evenly across the entire surface of the base metal, HAZ, and weld metal. The EDS spectrum in Figures 8 (e) and (f) only contain Fe, C, Si, O, and Cl for the first week of immersion, and the amount of the same composition we found after 8 weeks of immersion testing. Evidently, we discovered the amount of Cl$^-$ on the welded surface that roved the pitting corrosion containing the sodium cloride.

Figures 8 (a) and (b) depict changes in individual pit depth and surface area. Significant pits can be seen after 1-week immersion tests in NaCl solution. This is due to the fact that pitting initiation and growth have different mechanisms [11, 18-23].

Pit depth, pit area, and pit volume were among the individual pit characteristics that showed that the immersion surface pits were deeper than the salt-spray surface pits in relation to the surface morphology [18–21]. More pits formed on the immersion surface in relation to surface corrosion characteristics such as pit number density, pit surface area, nearest neighbour distance, and intergranular corrosion area fraction [14, 20-23]. The variations in pit features can be ascribed to the constant presence of water in the immersion environment surrounding the coupons. Pits were able to form and grow more quickly due to the removal of Fe from the entire surface area made possible by the presence of 3.5wt% NaCl.

4. CONCLUSION

The weight loss and corrosion rate demonstrate the corrosion behaviour on the welded joint, and SEM/ EDS analysis has been directed in the current work to study surface morphology after immersion testing. This paper reveals the significant uses of ER70s filler metal and low carbon steel base material for various applications, particularly in the oil and gas industry.

1. Microstructures obtained using an optical microscope show that the cross section of the weld metal consists of base material HAZ area and weld metal. The HAZ area has metallurgical changes that influence the higher Micro hardness value when compared to other areas.
2. The corrosion behaviour of welded joints was investigated in the absence and presence of 3.5wt.% NaCl. The weight loss and corrosion rate results from the immersion test showed that, despite being slightly higher in the NaCl medium compared to the non-NaCl medium, they were relatively low. In comparison to other areas, the HAZ area adjacent to low carbon steel has more severe uniform and localised corrosion.
3. The elemental composition of welded samples changed after SEM with EDX analysis. Only the composition of C, Si, Fe, and O was visible in the absence of NaCl, and Fe, Na, C, and O were revealed after immersion in salt solution.
4. It was suggested that a combination of ER70s filler metal and low carbon steel as the base material after welding performed better with the GMAW process based on changes in microstructure and micro hardness analysis. To reduce corrosion behaviour, control the changed HAZ area based on the welding parameter selection and geometry design.
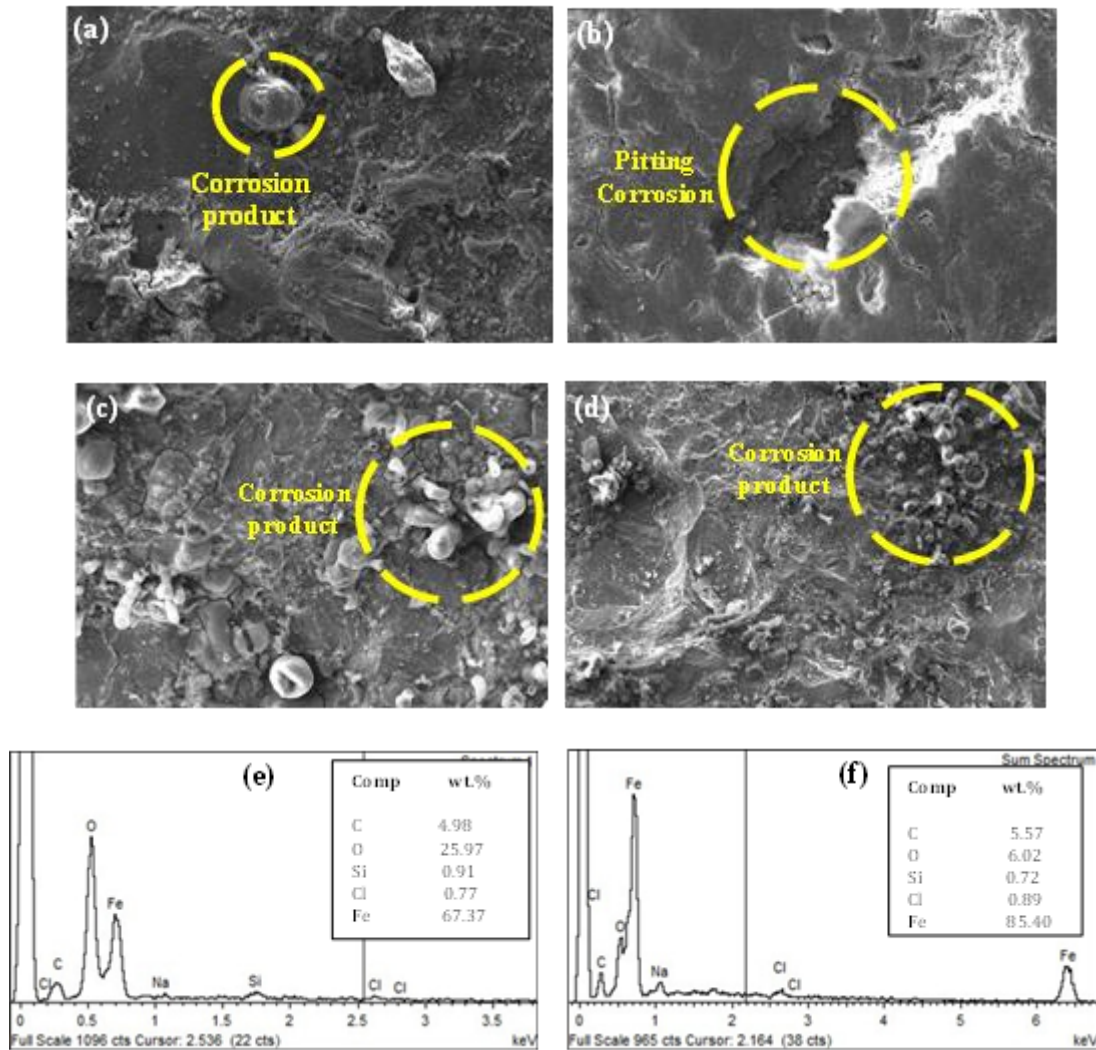
Figure 8. SEM morphology of sample immersed in 3.5wt. % NaCl solution (a) and (c) after 1 week, (b) and (d) after 8 weeks, (e) EDS analysis of sample (c) and (f) EDS analysis of sample (d).

REFERENCES

[1] A. R. Biswas, S. Chakraborty, P. S. Ghosh, and D. Bose, "Study of Parametric Effects on Mechanical Properties of Stainless Steel (AISI 304) and Medium Carbon Steel (45C8) Welded Joint Using GMAW, "Materials Today: Proceedings 5, no. 5 (2018) pp. 12384–12393, 2018.

[2] A. Aloraier, A. Albannai, A. Alaskari, M. Alawadhi, and S. Joshi, " TBW Technique by Varying Weld Polarities in SMAW as an Alternative to PWHT," International Journal of Pressure Vessels and Piping 194, no. PA: 104505, 2021.

[3] H. Dong, J. Yang, Y. Li, Y. Xia, X. Hao, P. Li, D. Sun, J. Hu, W. Zhou, and M. Lei, "Evolution of Interface and Tensile Properties in 5052 Aluminum Alloy/304 Stainless Steel Rotary Friction Welded Joint after Post- Weld Heat Treatment, "Journal of Manufacturing Processes 51, pp. 142– 150, 2020.

[4] I. A. Ibrahim, S. A. Mohamat, A. Amir, and A. Ghalib." The Effect of Gas Metal Arc Welding (GMAW) Processes on Different Welding Parameters." Procedia Engineering 41, pp. 1502–1506, 2012.

[5] U. S. Patil, and M. S. Kadam, "Microstructural Analysis of SMAW Process for Joining Stainless Steel 304 with Mild Steel 1018 and Parametric Optimization by Using Response Surface Methodology," Materials Today: Proceedings 44, pp. 1811–1815, 2021.

[6] W. Chuaiphan, and S. Loeshpah, "Evaluation of Microstructure, Mechanical Properties and Pitting Corrosion in Dissimilar of Alternative Low-Cost Stainless-Steel Grade 204Cu and 304 by GTA Welding Joint, "Journal of Materials Research and Technology 9, no. 3, pp. 5174–5183, 2020.

[7] E. Karadeniz., O. Ugur, and Y. Ceyhan Y. "The Effect of Process Parameters on Penetration in Gas Metal Arc Welding Processes, "Materials and Design 28, no. 2, pp. 649– 656, 2007.

[8] N. Kaewsakul, P. Rungsuk, and K. Kittipong, "The Effects of GMAW Parameters on Penetration, Hardness and Microstructure of AS3678-A350 High Strength Steel, "The International Journal of Advanced Culture Technology 3, no. 1, pp. 169–178, 2015.

[9] H. R. Ghazvinloo, A. Honarbakhsh-R., and N. Shadfar. " Effect of Arc Voltage, Welding Current and Welding Speed on Fatigue Life, Impact Energy and Bead Penetration of AA6061 Joints Produced by Robotic MIG Welding, " Indian Journal of Science and Technology 3, no. 2, pp. 156–162, 2010.

[10] T. E. Abioye., O. E. Ariwoola, T. I. Ogedengbe, P. K. Farayibi, and O. O. Gbadeyan, "Effects of Welding Speed on the Microstructure and Corrosion Behavior of Dissimilar Gas Metal Arc Weld Joints of AISI 304 Stainless Steel and Low Carbon Steel, "Materials Today: Proceedings 17, pp. 871–877, 2019.

[11] D. M. Shirinzadeh, J. Mohammadi, Y. Behnamian, A. Eghlimi, and A. Mostafaei. "Metallurgical Investigations and Corrosion Behavior of Failed Weld Joint in AISI 1518 Low Carbon Steel Pipeline, "Engineering Failure Analysis 53, pp. 78–96, 2015.

[12] M. F. Mamat, and E. Hamzah. "A Study on the Difference of Edge Design Shape and Corrosion Behavior for Low Carbon Steel Welded Joint Under Salt Fog Environment. no. 05, pp. 201–208, 2022.

[13] H. Park, P. Cheolho, L. Junghoon, N. Hyunbin, M. Byungrok, M. Younghoon, and K. Namhyun, "Microstructural Aspects of Hydrogen Stress Cracking in Seawater for Low Carbon Steel Welds Produced by Flux-Cored Arc Welding," Materials Science and Engineering A 820, no. June, pp. 141568, 2021.

[14] M. F. Mamat, and E. Hamzah, "Corrosion Behavior of Low Carbon Steel Welded Joint in NaCl Solution, "Advanced Materials Research. Vol. 845, pp. 173-177, 2014.

[15] G. Khalaj, and J. K. Mohammad, "Investigating the Corrosion of the Heat- Affected Zones (HAZs) of API-X70 Pipeline Steels in Aerated Carbonate Solution by Electrochemical Methods, "International Journal of Pressure Vessels and Piping 145, pp. 1–12, 2016.

[16] T. Singh, S. Arvinder, and S. Sumit, "Effect of Groove Design on the Mechanical Properties of Shielded Metal Arc Welded Joints, "Indian Journal of Science and Technology 12, no. 02, pp. 1–8, 2019.

[17] D. Pathak, P. S. Rudra, G. Sanjeev, and B. Vincent, "Influence of Groove Angle on Hardness and Reinforcement Height of Shielded Metal Arc Welded Joints for Low Carbon AISI 1016 Steel Plates, "Materials Today: Proceedings, Vol. 38, Part 1, pp. 40 – 43, 2021.

[18] S. P. Ambade, A. Sharma, A. P. Patil, Y. M. Puri, "Effect of Welding Processes and Heat Input on Corrosion Behaviour of Ferritic Stainless Steel 409M," Materials Today: Proceedings 41, pp. 1018–1023, 2021.

[19] O. S. I. Fayomi, O. D. Samuelb, M. Mashilo, A. P. Popoola, O. Agboola, andD. Balasubramanian, "Surface Effect of Environmentally Assisted Corrosion Growth of Automotive Welded Steel Performance," Materials Today: Proceedings 38, pp. 2380–2384, 2020.

[20] M. Alizadeh, S. Bordbar, "The Influence of Microstructure on the Protective Properties of the Corrosion Product Layer Generated on the Welded API X70 Steel in Chloride Solution," Corrosion Science 70: 170–179, 2013.

[21] M. N. Ilman, A. Widodo, and N. A. Triwibowo, "Metallurgical, mechanical and corrosion characteristics of vibration assisted gas metal arc AA6061-T6 welded joints," Journal of Advanced Joining Processes 6, pp. 100129, 2022.

[22] Z. Wan, W. Dai, W. Guo, Q. Jia, H. Zhang, J. Xue, L. Lin, and P. Peng, "Improved corrosion resistance of Ni-base Alloy 600 welded joint by laser shock peening," Journal of Manufacturing Processes 80, pp. 718–728, 2022.

[23] F. Gao, Z. Sun, S. Yang, Peng J., and Z. Liao, "Stress corrosion characteristics of electron beam welded titanium alloys joints in NaCl solution," Materials Characterization 192, pp. 112126, 2022.